

Kinetic and Mechanistic Studies of Sulfur Transfer from Imidomethylrhenium Sulfides

Wei-Dong Wang, Ilia A. Guzei,[†] and James H. Espenson*

Ames Laboratory and Department of Chemistry, Iowa State University of Science and Technology, Ames, Iowa 50011

Received January 29, 2002

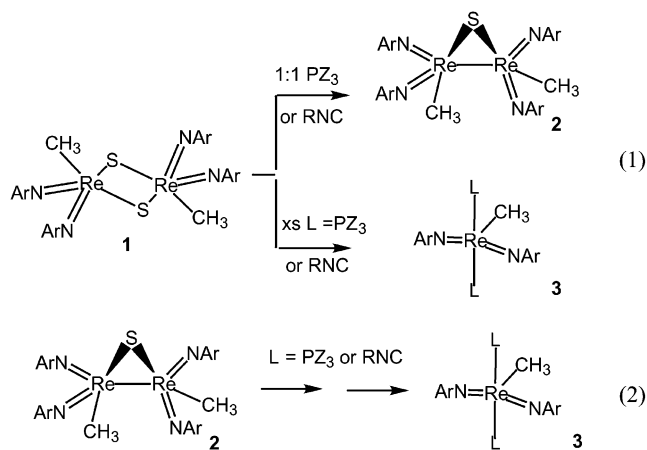
The bis(2,6-diisopropylphenylimido)methylrhenium(VII) sulfide dimer, $\{\text{CH}_3\text{Re}(\text{NAr})_2\}_2(\mu\text{-S})_2$ (**1**), reacts with a 1:1 amount of a phosphine or an alkyl isocyanide to yield a dimeric rhenium(VI) species, $\{\text{CH}_3\text{Re}(\text{NAr})_2\}_2(\mu\text{-S})$ (**2**), which has been structurally characterized. The two rhenium atoms in **2** are within bonding distance, 280 pm, more than 90 pm shorter than in **1**. With excess L, **1** reacts to give a monomeric rhenium(V) complex, $\text{CH}_3\text{Re}(\text{NAr})_2\text{L}_2$ (**3A**, L = PZ_3 , Z = alkyl, aryl; **3B**, L = isocyanide). The rate of formation of **3A** is *first-order* with respect to [**1**] and *second-order* with respect to monodentate phosphine concentrations. With bidentate phosphines, however, the order with respect to the phosphine drops to unity. The addition of another (nonoxidizable) coordinating ligand, such as pyridine or one of its derivatives, accelerates the formation of **3A**. In the presence of a pyridine ligand the reaction is first-order with respect to phosphine concentration, both monodentate and bidentate. The reactions between phosphines and **2** are slower than those with **1**, which excludes $[\text{CH}_3\text{Re}(\text{NAr})_2]_2(\mu\text{-S})$ from being the intermediate in the reactions of **1**. To account for that, we have proposed an intervening species that partitions between transformation to **3** with excess L and to **2** otherwise.

Introduction

Compared to the abundant reports on oxo-transfer reactions, relatively few studies have been published on the analogous sulfur-transfer processes.^{1–5} Rhenium(VII) and rhenium(V) complexes are believed to play important roles in the catalytic desulfurization of thiiranes.⁶ Here we report our studies on the sulfur transfer from rhenium(VII) and rhenium(VI) sulfido complexes to phosphines (PZ_3 , Z = alkyl, aryl) and isocyanides, eqs 1 and 2.

Experimental Section

Materials and Instrumentation. Unless stated otherwise, the phosphines and alkyl isocyanides used for this work were purchased from Aldrich or Strem, and used as received. Benzene (Aldrich), toluene- d_8 (Aldrich), and benzene- d_6 (CIL) were dried with sodium/



benzophenone and stored in a nitrogen-filled glovebox. The preparation of $\{\text{MeRe}(\text{NAr})_2\}_2(\mu\text{-S})_2$ (**1**, Ar = 2,6-diisopropylphenyl) has been reported previously.⁷ The synthesis of $\text{Me}_2\text{-PCH}_2\text{P}(\text{O})\text{Me}_2$ was adapted from the reported procedure.^{8,9} Phosphine disulfides $\text{Me}_2\text{P}(\text{S})(\text{CH}_2)_n\text{P}(\text{S})\text{Me}_2$ ($n = 1$ or 2) were prepared

* Author to whom correspondence should be addressed. E-mail: espenson@ameslab.gov.

[†] Current address: Department of Chemistry, University of Wisconsin, Madison, WI 53706.

(1) Woo, L. K. *Chem. Rev.* **1993**, 93, 1125.

(2) Berreau, L. M.; Woo, L. K. *J. Am. Chem. Soc.* **1995**, 117, 1314.

(3) Foley, S. R.; Richeson, D. S.; Darrin, S. *Chem. Commun.* **2000**, 1391.

(4) Young, C. G.; Laughlin, L. J.; Colmanet, S.; Scrofani, S. D. B. *Inorg. Chem.* **1996**, 35, 5368.

(5) Hall, K. A.; Mayer, J. M. *J. Am. Chem. Soc.* **1992**, 114, 10402.

(6) Jacob, J.; Espenson, J. H. *Chem. Commun.* **1999**, 1003.

(7) Wang, W.-D.; Guzei, I. A.; Espenson, J. H. *Inorg. Chem.* **2000**, 39, 4107.

(8) Mading, P.; Scheller, D. Z. *Anorg. Allg. Chem.* **1988**, 567, 179.

(9) Robertson, R. A. M.; Poole, A. D.; Payne, M. J.; Cole-Hamilton, D. J. *Chem. Commun.* **2001**, 47.

by mixing the bidentate phosphines with 2 equiv of sublimed sulfur in benzene, isolated as white precipitates and analyzed by comparison with the literature NMR data.^{8,10,11} A Bruker DRX-400 spectrometer was used to collect the ¹H, ¹³C, and ³¹P NMR spectra. The ¹H and ¹³C chemical shifts were measured relative to residual ¹H and ¹³C resonances in the deuterated solvents C₆D₅H ($\delta_{\text{H}} = 7.16$ ppm, $\delta_{\text{C}} = 128.39$ ppm) and C₆D₅CD₂H ($\delta = 2.09$ ppm). ³¹P chemical shifts were referenced to 85% H₃PO₄. Kinetics experiments were carried out under N₂ at 298 K by the use of a Shimadzu UV 3101PC equipped with a thermoelectrical cell holder. Elemental analyses were performed by Desert Analytics.

Kinetics. The stock solutions of {MeRe(NAr)₂}₂(μ -S)₂ (**1**) and {MeRe(NAr)₂}₂(μ -S) (**2**) in C₆H₆ were prepared and stored in a glovebox. All kinetic runs were performed with at least a 10-fold excess of phosphine or isocyanide over the rhenium complex. For more rapid reactions with PMe₃, dmpe, and dmpm, kinetic traces for the formation of CH₃Re(NAr)₂(PZ₃)₂ (**3A**) at 630 nm were recorded to >4 half-times. Equation 3

$$\text{Abs}_t = \text{Abs}_\infty + (\text{Abs}_0 - \text{Abs}_\infty) \times \exp(-k_p t)$$

was used to fit the absorbance–time data. For PMe₂Ph, the data were fit by the method of initial rates. The early stages of the absorbance–time curve at 629 nm ($\epsilon_3 = 1.2 \times 10^4$ L mol^{−1} cm^{−1}) were fit to the equation of a straight line; the slope of that line, Abs', was converted into the initial rate (in concentration units) by division by $\Delta\epsilon_3$ (1.2×10^4 L mol^{−1} cm^{−1}). None of the other species absorb at this wavelength, the difference in molar absorptivity between reactants and products at wavelength λ : $v_i = \text{Abs}'/\Delta\epsilon_\lambda$. Activation parameters were calculated over a temperature range of 283–313 K from the least-squares fit of values of $\ln(k/T)$ vs $1/T$, according to eq 4.

$$\ln\left(\frac{k}{T}\right) = \ln\left(\frac{k_B}{h}\right) + \frac{\Delta S^\ddagger}{R} - \frac{\Delta H^\ddagger}{RT} \quad (4)$$

Preparation of {MeRe(NAr)₂}₂(μ -S), **2.** To a 50 mL hexane solution of {CH₃Re(NAr)₂}₂(μ -S)₂ (100 mg, 0.0856 mmol) was added under nitrogen 12.2 μ L of PMe₂Ph (0.0856 mmol). The solution was stirred for 16 h, and then the solvent volume was reduced by vacuum to about 5 mL. The concentrated solution was cooled to −20 °C, yielding red crystals. NMR (C₆D₆, 298K): (¹H) δ 1.07 (d, $J = 8.8$ Hz, 12H), 1.10 (d, $J = 8.8$ Hz, 12H), 1.20 (d, $J = 8.8$ Hz, 24H), 3.41 (s, 3H), 3.45 (s, 3H), 3.69 (septet, $J = 8.8$ Hz, 4H), 3.89 (septet, $J = 8.8$ Hz, 4H), 7.0 (m, 12H); (¹³C) δ −4.72 (CH₃Re), 2.56 (CH₃Re). EI MS: m/z 1135. Anal. Found (Calcd for C₅₀H₇₄N₄Re₂S, FW = 1135.6): C, 52.64 (52.88); H, 6.46 (6.57); N, 4.85 (4.93); S, 2.76 (2.82).

Characterization of MeRe(NAr)₂L₂ (3**).** The structures and elemental analyses for L = dmpe and PMe₂Ph, as well as spectroscopic data for 10 analogous compounds, have been reported previously.¹² The corresponding dmpm and RNC complexes, unreported before, have spectroscopic data very similar to those of the fully characterized ones (see the Supporting Information).

MeRe(NAr)₂(dmpm)₂. NMR (C₆D₆, 298 K): (¹H) δ 7.14 (d, $J = 7$ Hz, 2H), 7.05 (d, $J = 7$ Hz, 2H), 6.92 (t, $J = 7$ Hz, 2H), 3.84 (septet, $J = 6.8$ Hz, 2H), 3.49 (septet, $J = 6.8$ Hz, 4H), 2.83 (t, $J = 4.6$ Hz, 3H, ReCH₃), 1.68 (m, 4H), 1.38 (br s, 12H), 1.36 (d, $J = 6.8$ Hz, 12H), 1.29 (d, $J = 6.8$ Hz, 12H), 0.66 (d, $J = 3.6$ Hz,

Table 1. Crystallographic Data for {MeRe(NAr)₂}₂(μ -S) (**2**, Ar = 2,6-Diisopropylphenyl)

empirical formula	C ₅₀ H ₇₄ N ₄ Re ₂ S	fw	1135.59
temp	173(2) K	l	0.71073 Å
cryst syst	triclinic	space group	<i>P</i> 1
unit cell	<i>a</i> = 10.9556(5) Å	unit cell	$\alpha = 105.780(1)^\circ$
dimensions	<i>b</i> = 13.4586(6) Å	dimensions	$\beta = 93.711(1)^\circ$
	<i>c</i> = 19.3160(9) Å		$\gamma = 112.715(1)^\circ$
vol	2481.5 (2) Å ³	Z	2
density(calcd)	1.520 g/cm ³	m	49.51 cm ^{−1}
F ₀₀₀	1136		
R ^a	0.0231	R _w ^a	0.0484

$$^a R(wF^2) = \Sigma[w(F_o^2 - F_c^2)]/\Sigma[w(F_o^2)^2]^{1/2}. R = \Sigma\Delta/\Sigma(F_o). \Delta = |(F_o - F_c)|.$$

12H); (¹³C) δ −31.0 (ReCH₃); (³¹P) δ −23.3 (virtual t, $J = 10.8$ Hz), −57.9 (t, $J = 10.8$ Hz).

MeRe(NAr)₂(CNⁿBu)₂. NMR (C₆D₆, 280 K): (¹H) δ 7.18 (m, 4H), 6.97 (t, $J = 7$ Hz, 2H), 3.88 (septet, $J = 6.8$ Hz, 4H), 2.91 (s, 3H, ReCH₃), 1.47 (d, $J = 6.8$ Hz, 24H), 0.74 (s, 18H); (¹³C) δ −29.1 (ReCH₃).

MeRe(NAr)₂(CNⁿBu)₂. NMR (C₆D₆, 283 K): (¹H) δ 6.9–7.2 (6H), 3.94 (septet, $J = 6.8$ Hz, 4H), 2.96 (s, 3H, ReCH₃), 2.66 (t, $J = 6$ Hz, 4H), 0.8 (m, 8H), 0.47 (t, $J = 6$ Hz, 6H); (¹³C) δ −29.0 (ReCH₃).

X-ray Crystallography. A yellow crystal of **2** with approximate dimensions 0.35 × 0.25 × 0.24 mm³ was selected under oil. The crystal was mounted to the tip of a glass capillary in a stream of cold nitrogen at 173 K and centered in the X-ray beam by using a video camera. The data collection was performed on a Bruker CCD-1000 diffractometer with Mo K α ($\lambda = 0.71073$ Å) radiation. The final cell constants were calculated from a set of 5360 strong reflections from the actual data collection. The data were collected by using the hemisphere data collection routine. The reciprocal space was surveyed to the extent of 1.9 hemispheres to a resolution of 0.80 Å. A total of 22192 data were harvested by collecting three sets of frames with 0.3° scans in ω with an exposure time 30 s per frame. These highly redundant datasets were corrected for Lorentz and polarization effects. The absorption correction was based on fitting a function to the empirical transmission surface as sampled by multiple equivalent measurements.¹³

The systematic absences in the diffraction data were consistent for the space groups *P*1 and $\bar{P}1$.¹⁴ The *E*-statistics strongly suggested the centrosymmetric space group $\bar{P}1$ that yielded chemically reasonable and computationally stable results of refinement. A successful solution by direct methods provided most non-hydrogen atoms from the *E*-map. The remaining non-hydrogen atoms were located in an alternating series of least-squares cycles and difference Fourier maps. All non-hydrogen atoms were refined with anisotropic displacement coefficients. All hydrogen atoms were included in the structure factor calculation at idealized positions and were allowed to ride on the neighboring atoms with relative isotropic displacement coefficients. The final least-squares refinement of 533 parameters against 10037 data resulted in residuals *R* (based on *F*² for $I \geq 2\sigma$) and *R*_w (based on *F*² for all data) of 0.0231 and 0.0484, respectively. Crystallographic data for **2** are given in Table 1.

Results

Reactions with Phosphines. When a *stoichiometric amount* of PMe₂Ph was used to react with **1**, the color of

(10) Maeding, P. Z. Chem. 1986, 26, 408.

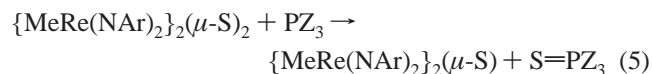
(11) Karsch, H. H. Chem. Ber. 1982, 115, 818.

(12) Wang, W.-D.; Guzei, I. A.; Espenson, J. H. Organometallics 2001, 20, 148.

(13) Blessing, R. H. Acta Crystallogr., A 1995, 51, 33.

(14) All software and sources of the scattering factors are contained in the SHELXTL (version 5.1) program library (G. Sheldrick, Bruker Analytical X-ray Systems, Madison, WI).

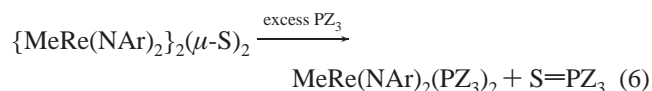
the C_6D_6 solution slowly changed from green-brown to the orange-red color characteristic of **2**. At completion, only the free $\text{S}=\text{PMe}_2\text{Ph}$ at 31.2 ppm was observed in the ^{31}P NMR spectrum. The ^1H NMR spectrum showed two singlets at 3.45 and 3.41 ppm with the same intensity; the corresponding ^{13}C chemical shifts were at 2.56 and -4.72 ppm, respectively. These resonances were assigned to the two *inequivalent* methyl groups bound to the rhenium atoms of **2**. There were also two sets of septets from the methine protons of the arylimido groups, which a ^1H – ^1H 2D-COSY experiment showed were coupled to three doublets of the methyl protons of isopropyl moieties at ~ 1 ppm. Other phosphines, such as PMe_3 , dmpe, and dmpm, also led to identical ^1H and ^{13}C NMR spectra for rhenium product **2**. On the basis of the intensities of the ^1H signals and the lack of indication of phosphine binding, the rhenium product of the reactions between **1** and an equimolar amount of phosphine (with an excess, further reaction ensued) was formulated as $\{\text{MeRe}(\text{NAr})_2\}_2(\mu\text{-S})$ (**2**), eq 5.



The presence of a single sulfur atom in **2** is consistent with the elemental analysis and the EI mass spectrum. The inequivalent methyl groups as shown in the NMR spectra suggest that the two rhenium centers are found in different chemical environments. This has been confirmed by the X-ray diffraction studies, as presented subsequently. Unexpectedly, the chemical shifts of the two rhenium methyl protons approached one another as the temperature decreased. For example, the chemical shift difference in C_7D_8 was 0.082 ppm at 323 K, but dropped to 0.027 ppm at 283 K. The two singlets merged into a single resonance at 263 K. When the temperature was decreased further, two singlets reappeared. The variable-temperature NMR data suggest that the two methyl groups remain inequivalent through the above-mentioned temperature range and the Re–Re bond is likely intact.

Compound **2** and phosphine sulfide were also formed with $\text{P}(\text{OMe})_3$, $\text{P}(\text{OMe})_2\text{Ph}$, $\text{P}(\text{OMe})\text{Ph}_2$, PMePh_2 , and $\text{P}(\text{Pr})_3$. With these phosphines, but not the ones given before, **2** persists long enough to be observed *even in the presence of excess phosphine*. No reaction between **1** and an excess of PPh_3 or PCy_3 was observed in 2 days at room temperature.

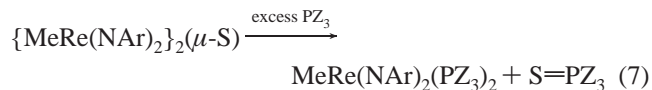
When PMe_2Ph was added in ≥ 10 -fold excess to a C_6D_6 solution of **1**, the color of the solution changed to the intense green characteristic of **3A**. Compound **2** was not observed; however, ^1H and ^{31}P NMR spectra indicated that the structurally characterized compound $\text{MeRe}(\text{NAr})_2(\text{PMe}_2\text{Ph})_2$ was produced.¹² Similar products $\text{MeRe}(\text{NAr})_2(\text{PZ}_3)_2$ (**3A**) were also observed when excesses of PMe_3 , dmpe, and dmpm were used, eq 6.



The molecular structure of the dmpe product **3A** was reported

previously, establishing that dmpe acts as a monodentate ligand.¹² Only one of its phosphorus atoms is coordinated to rhenium, and the two dangling bifunctional phosphines lie trans to each other. As in the case of the dmpe analogue, the dmpm product also showed two virtual triplets in the ^{31}P NMR spectrum. The triplet at -23.6 ppm coupled with the triplet at -59.7 ppm as revealed by the ^{31}P – ^{31}P 2D experiment. The virtual triplet pattern of the ^{31}P resonances of the dmpm product did not change as the magnetic field changed from 81 to 202 MHz. For both dmpe and dmpm, the phosphine products were $\text{Me}_2\text{P}(\text{S})(\text{CH}_2)_n\text{PMe}_2$ ($n = 1, 2$); the possible disulfide products $\text{Me}_2\text{P}(\text{S})(\text{CH}_2)_n\text{P}(\text{S})\text{Me}_2$ were not observed. The reaction of **1** with an excess of $\text{Me}_2\text{P}(\text{O})\text{CH}_2\text{PMe}_2$ yielded a **3A**-type $\text{Re}(\text{V})$ species and $\text{Me}_2\text{P}(\text{O})\text{CH}_2\text{P}(\text{S})\text{Me}_2$. Detailed spectroscopic data are given in the Supporting Information.

Certain control experiments were performed to demonstrate the lack of S–P redistribution reactions between real or potential $\text{P}=\text{S}$ products. It was shown that the sulfur transfer between dppe and $\text{Me}_2\text{P}(\text{S})\text{CH}_2\text{CH}_2\text{P}(\text{S})\text{Me}_2$ or $\text{S}=\text{PMe}_2\text{Ph}$ did not occur under the experimental conditions, whether potential rhenium catalysts were absent or not. Compound **3A** was also observed when excess dmpe, dmpm, $\text{P}(\text{OMe})_2\text{Ph}$, PMe_3 , or PMe_2Ph was added to a solution of **2**, eq 7. However, no further reaction between **2** and an excess of PMePh_2 was observed in 2 days at room temperature. The reaction of **2** and $\text{P}(\text{OMe})_3$ was also very sluggish.



Reactions with Isocyanides. Like phosphines, alkyl isocyanides RNC ($\text{R} = {}^n\text{Bu}$ and ${}^t\text{Bu}$) react with 1 equiv of **1** to yield RNCS and **2**, both of which were identified by their ^1H and ^{13}C NMR resonances. When excess RNC was used to react with **1**, or more RNC was added to a solution of **2**, the compound $\text{MeRe}(\text{NAr})_2(\text{CNR})_2$, **3B**, was recognized from its spectroscopic similarities to **3A**. Specifically, the electronic spectrum of the deep blue-green colored $\text{MeRe}(\text{NAr})_2(\text{CN}^t\text{Bu})_2$ also showed an intense band at 609 nm ($\epsilon_{\text{3B}} = 1.5 \times 10^4 \text{ L mol}^{-1} \text{ cm}^{-1}$), paralleling the 580–630 nm band of **3A**. For the ${}^t\text{BuNC}$ product, the sharp singlet at 2.91 ppm in the ^1H NMR spectrum with a corresponding ^{13}C chemical shift at -29.1 ppm assigned to the methyl group bound to rhenium was characteristic of $\text{CH}_3\text{Re}(\text{NAr})_2(\text{L})_2$ (**3**) complexes. At 280 K, the resonances for the free and coordinated ${}^t\text{BuNC}$ ligand at 0.85 and 0.74 ppm, respectively, were noticeably broader than that for ${}^t\text{BuNCS}$ at 0.77 ppm. The NAr groups exhibited a septet and a doublet at 3.88 and 1.47 ppm with the same coupling constant of 6.8 Hz. The integrations for the rhenium methyl, coordinated ${}^t\text{BuNC}$, and NAr moieties were consistent with the formula of $\text{MeRe}(\text{NAr})_2(\text{CN}^t\text{Bu})_2$. The ^1H NMR resonance of the $\text{Re}-\text{CH}_3$ group shifted from 2.91 ppm in C_6D_6 at 280 K to 2.79 ppm at 320 K.

Addition of PMe_2Ph or dmpe to the solution of $\text{MeRe}(\text{NAr})_2(\text{CN}^t\text{Bu})_2$ yielded **3A** and free isocyanide. Ligand substitution was also observed with $\text{P}(\text{OMe})_3$. Qualitatively,

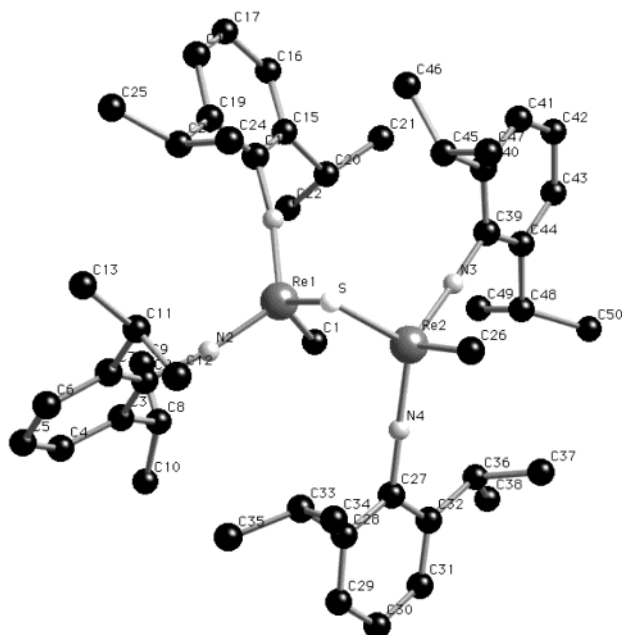


Figure 1. An ORTEP view of the molecular structure of $\{\text{MeRe}(\text{NAr})_2\}_2(\mu\text{-S})$ (**2**, Ar = 2,6-diisopropylphenyl) with thermal ellipsoids at the 30% probability level.

Table 2. Selected Bond Lengths (pm) and Bond Angles (deg) for $\{\text{MeRe}(\text{NAr})_2\}_2(\mu\text{-S})$ (**2**, Ar = 2,6-Diisopropylphenyl)

Re(1)–Re(2)	279.74(2)	Re(2)–S	228.93(9)
Re(1)–N(1)	173.8(3)	Re(2)–N(3)	176.2(3)
Re(1)–N(2)	174.9(3)	Re(2)–N(4)	176.1(3)
Re(1)–C(1)	214.4(3)	Re(2)–C(26)	213.9(4)
Re(1)–S	229.65(9)		
Re(1)–S–Re(2)	75.18(3)	N(1)–Re(1)–C(1)	99.47(13)
S–Re(1)–Re(2)	52.29(2)	N(1)–Re(1)–S	107.00(9)
N(1)–Re(1)–N(2)	121.35(13)	N(3)–Re(2)–N(4)	129.83(13)
C(1)–Re(1)–Re(2)	75.79(10)	C(26)–Re(2)–Re(1)	134.93(11)
Re(1)–N(1)–C(14)	170.4(2)	Re(2)–N(3)–C(39)	175.8(4)
Re(1)–N(2)–C(2)	169.0(2)	Re(2)–N(4)–C(27)	176.4(3)

the binding abilities of $^t\text{BuNC}$ and $\text{P}(\text{OMe})_3$ toward $\text{Re}(\text{V})$ are of the same order of magnitude. Unlike most of the phosphine analogues, only one set of isopropyl groups in $\text{MeRe}(\text{NAr})_2(\text{CN}^t\text{Bu})_2$ was observed even in C_7D_8 at 243 K. We suggest that their equivalence arises from fast rotation along the (Ar)C–N bond as a result of the isocyanide ligand being less sterically demanding than phosphine.

Neither $^t\text{BuNC}$ nor $^t\text{BuNC}$ reacts with $\text{MeRe}(\text{NAr})_2\text{O}$. For example, addition of 10 mM $\text{MeRe}(\text{NAr})_2\text{O}$ and 10 mM $^t\text{BuNC}$ led only to the formation of equilibrated amounts of $\text{MeRe}(\text{NAr})_3$ and $\text{MeRe}(\text{NAr})\text{O}_2$ after 10 days at room temperature in C_6D_6 . The formation of $^t\text{BuNCO}$ was not observed.

Structure of 2. The molecular structure of $\{\text{MeRe}(\text{NAr})_2\}_2(\mu\text{-S})$ (**2**) is given in Figure 1. Unlike the asymmetric bisulfido bridges in $\{\text{MeRe}(\text{NAr})_2\}_2(\mu\text{-S})_2$ (**1**),⁷ the mono-sulfido bridge in **2** is symmetric between the two rhenium centers with the Re–S bond distance at 229.6 pm. Therefore, the rhenium atoms in **2** may better be viewed as $\text{Re}(\text{VI})$ instead of one $\text{Re}(\text{V})$ and one $\text{Re}(\text{VII})$, such that the unpaired electron on each rhenium interacts to form a Re–Re single bond. The distance between the two rhenium atoms in **2** is 279.7 pm, which is much shorter than the 371.9 pm distance

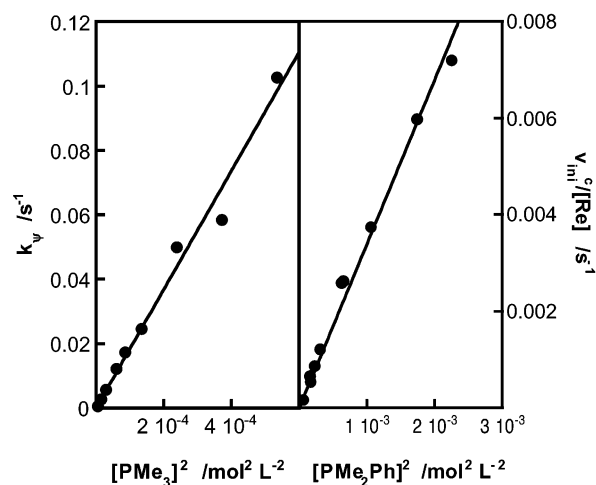


Figure 2. Second-order dependences of the pseudo-first-order rate constant (PMe_3) and the rhenium-normalized initial rate (PMe_2Ph) for reactions of **1** on the concentrations of these monodentate phosphines in benzene at 298 K.

in **1**. It should be noted that the two rhenium centers are not chemically equivalent even though the sulfido bridge is symmetric. The methyl group on one rhenium is pointing away from the other rhenium, while the other methyl group is pointing toward the neighboring rhenium. The different environments in which the two methyl groups reside may result in the peculiar ^1H chemical shift changes in the variable-temperature studies. Selected bond distances and angles are given in Table 2.

The analogous $\mu\text{-O}$ complex $\{\text{MeRe}(\text{NAr})_2\}_2(\mu\text{-O})$ has previously been structurally characterized.¹² As expected, the Re–Re distance in the $\mu\text{-O}$ case is shorter than that in **2**, 268.4 vs 279.7 pm, respectively. Also resulting from the size difference of oxygen and sulfur, the O–Re–Re angle is about 6° less than the S–Re–Re angle. The remarkable difference between the two compounds is the arrangement of the two methyl groups. The oxo compound adopts a syn,syn arrangement. On the other hand, the sulfido complex exists in a syn,anti arrangement with C_s symmetry. ^1H NMR studies in the range 243–323 K showed no indication of a syn,anti to syn,syn conversion for the $\mu\text{-S}$ compound. Even at 263 K, when the two methyl proton resonances merged into one, there were still two resonances for the methine protons of the isopropyl groups, in contrast to one methyl resonance and one methine resonance observed for the $\mu\text{-O}$ complex. The reversibility of the variable-temperature spectra also excludes the possibility of a process involving kinetic and thermodynamic isomers.

Kinetics. The initial rate method was used to study the reaction between **1** and PMe_2Ph . The formation of $\text{MeRe}(\text{NAr})_2(\text{PMe}_2\text{Ph})_2$ was monitored at 629 nm ($\epsilon_3 = 1.2 \times 10^4 \text{ L mol}^{-1} \text{ cm}^{-1}$), with **1** and $[\text{PMe}_2\text{Ph}]$ varied in the ranges 0.1–0.5 and 7–50 mM, respectively. The initial rate was first-order with respect to **1**, but second-order with respect to $[\text{PMe}_2\text{Ph}]$, Figure 2 and eq 8. The slope of the plot of $v_i/[\text{1}]$ against $[\text{PMe}_2\text{Ph}]^2$ yielded a third-order rate constant, $k_m = 3.3(1) \text{ L}^2 \text{ mol}^{-2} \text{ s}^{-1}$. Full kinetic profiles were collected for reactions with 32 and 42 mM PMe_2Ph . The traces fitted eq 3 exactly, and $k = 3.4 \text{ L}^2 \text{ mol}^{-2} \text{ s}^{-1}$ was obtained. The

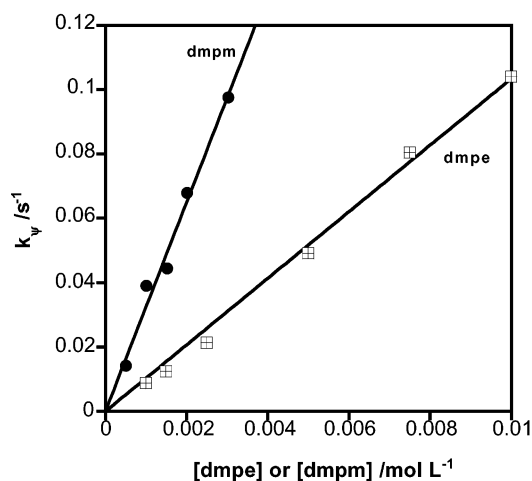


Figure 3. Pseudo-first-order rate constants in benzene at 298 K for the reactions of $\{\text{MeRe}(\text{NAr})_2\}_2(\mu\text{-S})_2$ (**1**, Ar = 2,6-diisopropylphenyl) against the concentrations of bifunctional phosphines showing that these reactions are first-order with respect to [dmpe] and [dmpm].

Table 3. Summary of Rate Constants^a for the Reactions of Phosphines with $\{\text{MeRe}(\text{NAr})_2\}_2(\mu\text{-S})_2$ (**1**) and $\{\text{MeRe}(\text{NAr})_2\}_2(\mu\text{-S})$ (**2**)

L	1		2
	k_m	k_b	k_2
PMe ₃	184(7)		0.195(3)
PMe ₂ Ph	3.3(1)		0.017(1)
Me ₂ P(O)CH ₂ PMe ₂	2.15(4)		0.080(9)
dmpe		10.3(2) ^a	0.108(2)
dmpm		32.5(10) ^a	0.070(3)
<i>tert</i> -butyl isocyanide	0.082(2)		^b

^a Units: k_m , L² mol⁻² s⁻¹; k_b and k_2 , L mol⁻¹ s⁻¹. ^b Not determined.

reaction of **1** with PMe₃ was faster than that with PMe₂Ph, and kinetic traces for the entire time course were collected. The plot of k_p against $[\text{PMe}_3]^2$, Figure 2, gave $k = 184(7)$ L² mol⁻² s⁻¹. As with other monodentate phosphines, the reaction of **1** with Me₂P(O)CH₂PMe₂ studied by the use of the initial rate method was directly proportional to $[\text{Me}_2\text{P}(\text{O})\text{CH}_2\text{PMe}_2]^2$. The reactions of **1** with the bifunctional phosphines dmpe and dmpm show first-order dependences on their concentrations, Figure 3 and eq 9. The two rate equations are given in eqs 8 and 9, and the rate constants k_m and k_b are summarized in Table 3.

$$-d[\mathbf{1}]/dt = k_m[\mathbf{1}][\text{PZ}_3]^2 \quad (\text{monodentate phosphine}) \quad (8)$$

$$-d[\mathbf{1}]/dt = k_b[\mathbf{1}][\text{Ph}_2\text{P}(\text{CH}_2)_n\text{PPh}_2] \quad (\text{bidentate phosphine}) \quad (9)$$

The reaction between **2** and a large excess of PMe₃ fit single-exponential kinetics exactly. The pseudo-first-order plot, Figure 4, clearly showed that the reaction with **2** was first-order with respect to [PMe₃]. The same rate law holds for PMe₂Ph, dmpe, and dmpm, as shown in Figure 4. The second-order rate constants from least-squares fitting are given in Table 3. The rate equation is

$$-d[\mathbf{2}]/dt = k_2[\mathbf{2}][\text{any phosphine}] \quad (10)$$

Phosphine Reactions in the Presence of Pyridine. Unlike the case of CH₃ReO₃,¹⁵ the chemical shift of the CH₃ protons

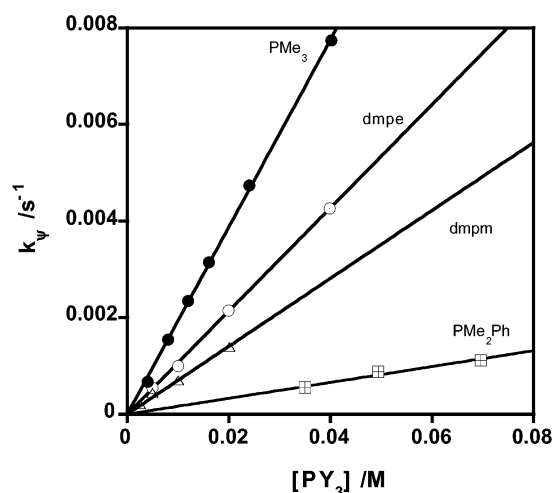


Figure 4. k_p against $[\text{PZ}_3]$ for the reactions between $\{\text{MeRe}(\text{NAr})_2\}_2(\mu\text{-S})_2$ (**2**, Ar = 2,6-diisopropylphenyl) and phosphines; both monodentate and bidentate phosphines show first-order dependences.

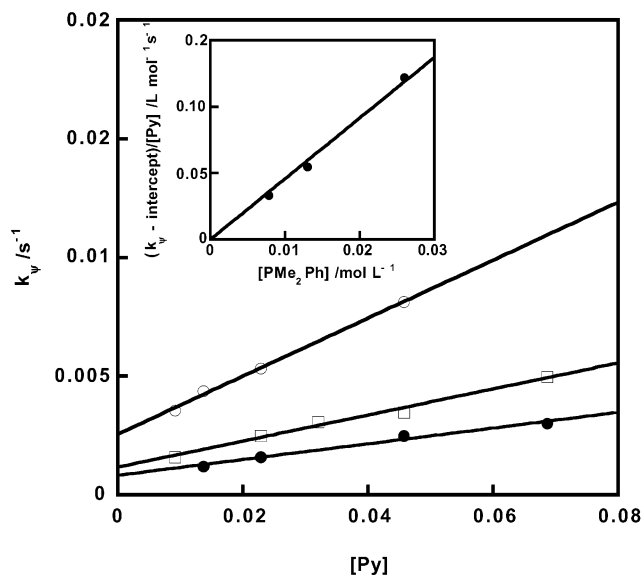


Figure 5. Effects of $[\text{Py}]$ on the reaction between **1** and PMe₂Ph in C₆H₆ at 298 K. The intercept is a function of $k_1[\text{PMe}_2\text{Ph}]^2$; see the text. Conditions: $[\mathbf{1}] = 0.045$ mM; open circles, $[\text{PMe}_2\text{Ph}] = 26$ mM; squares, $[\text{PMe}_2\text{Ph}] = 13$ mM; solid circles, $[\text{PMe}_2\text{Ph}] = 7.8$ mM. The inset shows that the slopes are first-order with respect to $[\text{PMe}_2\text{Ph}]$.

bound to Re in **1** did not change upon addition of pyridine, indicating a weak interaction. However, pyridine did show an effect on the reaction of **1** with PMe₂Ph. When $[\text{PMe}_2\text{Ph}]$ was kept constant at 7.8, 13, or 26 mM, the observed first-order rate constant for the formation of **3** was linearly proportional to $[\text{Py}]$ in the range 9–68 mM, Figure 5. The slopes of the straight lines were a linear function of $[\text{PMe}_2\text{Ph}]$; see the Figure 5 inset. The above results and those in the absence of pyridine could be described by eq 11.

$$k_p = k_m[\text{PMe}_2\text{Ph}]^2 + k_m'[\text{PMe}_2\text{Ph}][\text{Py}] \quad (11)$$

The unmistakable intercept in Figure 5 arises from the first term of eq 11. The computer program Scientist was used to

(15) Wang, W.-D.; Espenson, J. H. *J. Am. Chem. Soc.* **1998**, *120*, 11335.

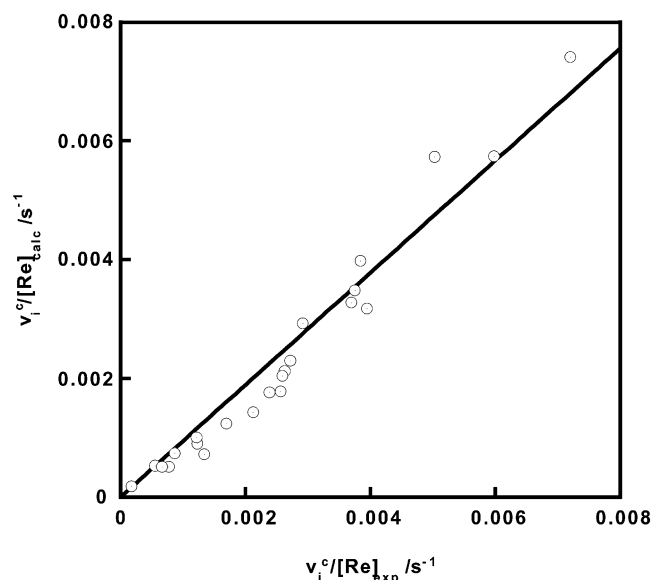


Figure 6. Agreement between kinetic data fitted to the rate law in eq 11 versus experimental kinetic data.

Table 4. Activation Parameters for Reactions between dmpm and Sulfidorhenium Compounds

	$\Delta S^\ddagger/\text{J mol}^{-1} \text{ K}^{-1}$	$\Delta H^\ddagger/\text{kJ mol}^{-1}$
$\{\text{MeRe}(\text{NAr})_2\}_2(\mu\text{-S})_2$ (1)	175(4)	13(1)
$\{\text{MeRe}(\text{NAr})_2\}_2(\mu\text{-S})$ (2)	133(7)	40(2)

carry out the multivariate data analysis. The values obtained are $k_m = 3.3(1) \text{ L}^2 \text{ mol}^{-2} \text{ s}^{-1}$ (which agrees with the entry in Table 3) and $k_m' = 3.4(2) \text{ L}^2 \text{ mol}^{-2} \text{ s}^{-1}$. The plot of the calculated values of k_p obtained from the best fit to eq 11 against the experimental ones is shown in Figure 6. The accelerating effect was also observed in the presence of 4-methoxypyridine. It is worth noting that the observed rate constant for the reaction of **1** with 1.5 mM dmpm in the presence of 24 mM Py is the same as the value in the absence of Py. On the other hand, 4-(dimethylamino)pyridine ranging from 15 to 150 mM did speed up the reaction with dmpm. Product **3A** is stable toward these pyridines, but unstable toward 2-dimethylaminoaniline.

As expected, the formation of **3B** from the reaction of **1** with $^t\text{BuNC}$ also took place with a second-order dependence on $^t\text{BuNC}$. The observed rate constants were 1.9×10^{-3} and $2.7 \times 10^{-4} \text{ s}^{-1}$ when the concentrations of the excess reagent of $^t\text{BuNC}$ were 0.15 and 0.058 mol L^{-1} , respectively. Thus, the third-order rate constant is $8.2(2) \times 10^{-2} \text{ L}^2 \text{ mol}^{-2} \text{ s}^{-1}$.

Temperature Profiles. The temperature dependence of the reactions of **1** and **2** with dmpm was studied in a temperature range of 283–313 K. Activation parameters were calculated from the least-squares fit of values of $\ln(k/T)$ to $1/T$, according to eq 4. The resulting activation enthalpies for dppm were $\Delta H_b^\ddagger = 13(1) \text{ kJ mol}^{-1}$ and $\Delta H_2^\ddagger = 40(2) \text{ kJ mol}^{-1}$ for the reaction with **1** and **2**, respectively. Both reactions proceed with large negative activation entropies, Table 4.

Discussion

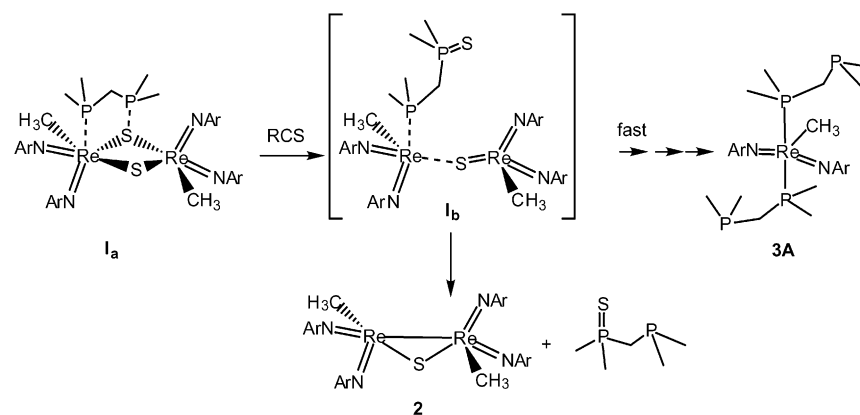
Kinetics and Mechanisms. For monodentate phosphines PZ_3 (PMe_3 or PMe_2Ph), the rate of formation of **3A** from **1**, eq 1, is second-order with respect to $[\text{PZ}_3]$, but first-order with respect to $[\text{PZ}_3]$ for reaction 2 when **2** affords **3**. Though one cannot directly compare the rate constants with different units, under the experimental conditions the formation of **3A** from **1** is clearly faster than that from **2**, on the basis of the rates at which the changes in the UV/vis spectra occur. For bidentate phosphines PP (dmpm or dmpm), the formation of **3A** is first-order with respect to $[\text{PP}]$ regardless of whether the reaction starts with **1** or **2**. The rate constants for the reactions of dmpm and dmpm with **1** are at least 100 times larger than those with **2**. Again, it seems unlikely that compound **2** is the intermediate toward the formation of **3A** for the reactions of **1** with excess phosphines. To account for the kinetic observations, we propose the mechanism presented in Scheme 1. The phosphorus atoms of the bidentate ligands interact with the rhenium and sulfur atoms of **1** to form a five-membered ring for dmpm (shown in the scheme as **I_a**) and an analogous six-membered ring intermediate for dmpm. Note that one P donor atom attacks the $\mu\text{-S}$ group of **1** and the other P donor is coordinated to Re. The finding that Py acts as a stand-in for the second monodentate phosphine allows us to argue that the second P donor does not attack the second $\mu\text{-S}$ group. The possibility that the two phosphorus atoms interact with the two sulfur atoms was additionally ruled out on the basis that phosphine disulfides $\text{Me}_2\text{P}(\text{S})(\text{CH}_2)_n\text{P}(\text{S})\text{Me}_2$ are absent; only $\text{Me}_2\text{P}(\text{S})(\text{CH}_2)_n\text{PMe}_2$ was obtained, combined with our experimental evidence showing the absence of $\text{P}=\text{S}$ redistribution.

An intermediate containing $\text{Re(V)}\text{--Re(VII)}$ (**I_b**) is subsequently formed. The remaining steps, ligand substitution and terminal sulfur transfer, are thought to be faster. The kinetic and spectroscopic data are in accord with this. For monodentate phosphines or a bidentate phosphine with one of the binding sites blocked by oxidation of one phosphine to its oxide, a second phosphine is needed to form the **I_a**-like intermediate. This proposal accounts for the second-order dependence on $[\text{Me}_2\text{P}(\text{O})\text{CH}_2\text{PMe}_2]$. Neither **I_a** nor **I_b** was detected; however, a $\text{Re(V)}\text{--Re(VII)}$ intermediate, $\text{Me}(\text{NAr})_2\text{Re}\text{--ORe}(\text{NAr})_2\text{Me}$, was observed for the reaction of $\text{MeRe}(\text{NAr})_2\text{O}$ with phosphines.¹² When phosphine is limiting in concentration or when a less nucleophilic phosphine is used, a competition reaction that leads to the formation of **2** occurs.

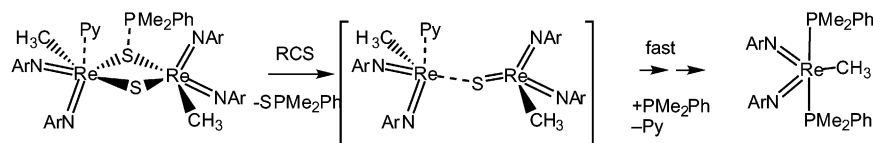
When sulfur transfer was carried out in the presence of pyridine, further rate acceleration was observed. Because there is no observable interaction between **1** and pyridine was observed, it is likely that the phosphine attack at the sulfur atom is the initial step. The pyridine is believed to coordinate to rhenium. The modified reaction scheme is presented in Scheme 2.

Though it is known that sulfur transfer between phosphorus centers occurs at elevated temperatures, it does not happen during these reactions. Tests showed that S re-

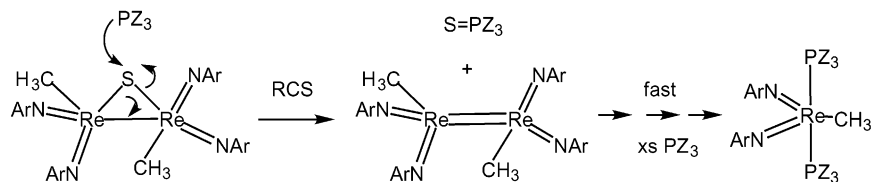
Scheme 1



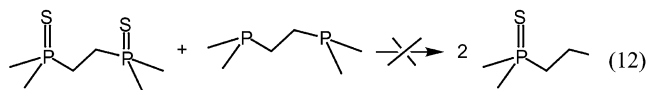
Scheme 2



Scheme 3



distribution between Me₂PCH₂CH₂PMe₂ and Me₂P(S)CH₂CH₂P(S)Me₂ did not occur under the experimental conditions. This finding makes the point that the disulfide is not an initial reaction product that is later converted to the observed monosulfide.



A proposed mechanism involving a dimeric intermediate for the reactions of **2** with phosphines is given in Scheme 3. The sulfur-transfer step is believed to be rate controlling. Attempts to prepare the CH₃(NAr)₂Re=Re(NAr)₂CH₃ intermediate by using a limiting amount of phosphine failed. An alternative to this has the reaction occurring via two three-coordinate Re(V) intermediates. Cummins and others have prepared a number of three-coordinate compounds with sterically hindered amino ligands.^{16–18} When the substituents were not sufficiently large, a dimer was obtained. For example, the dimer Mo₂(NMe₂)₆ was isolated,¹⁹ but a monomer, Mo[N(R')(Ar')]₃, formed with the *tert*-butyl(3,5-

dimethylphenyl)amino ligand.^{20,21} Williams and Schrock have isolated a number of three-coordinate nearly trigonal planar Re(V) anions and structurally characterized the bis(tri-phenylphosphoranylidene)ammonium (PPN⁺) salt of Re(NAr)₃[–]. It is interesting to note that the nucleophilic Re(NAr)₃[–] can be alkylated and protonated to yield MeRe(NAr)₃ and HRe(NAr)₃, respectively. For mercuric ion, X-ray studies showed the crystal structure with a molecular unit of (ArN)₃Re–Hg–Re(NAr)₃.²² As in the reactions with **1**, no intermediate—neither the Re(V) dimer nor the three-coordinate Re(V) monomer—was observed. Pyridine acceleration was observed only in the reactions of **1**, not **2**, possibly because the Re–Re distance in **2** is about 90 pm shorter than in **1**, leading to additional steric crowding. Attack of PZ₃ at the μ -S group of **2** is being proposed, because (a) the product is phosphine sulfide and (b) pyridine does not convert **2** to MeRe(NAr)₂Py₂, analogous to **3**.

Comparison of Oxo- and Sulfur-Transfer Structures. Compound **2** adopts the anti,syn arrangement, whereas its μ -O counterpart **4** was characterized as syn,syn.¹² A long-lived intermediate with the same molecular formula was detected as preceding **4**.¹² Its ¹H and ¹³C NMR spectra consisted of resonances from *two* ReMe groups, *two* ArCHMe₂ septets, and *four* ArCHMe₂ doublets. On that basis, structure **5** was suggested. A reviewer of this paper has added another

(16) Cummins, C. C. *Chem. Commun.* **1998**, 1777.

(17) Alyea, E. C.; Basi, J. S.; Bradley, D. C.; Chisholm, M. H. *Chem. Commun.* **1968**, 495.

(18) Alyea, E. C.; Bradley, D. C.; Copperthwaite, R. G. *J. Chem. Soc., Dalton Trans.* **1972**, 1580.

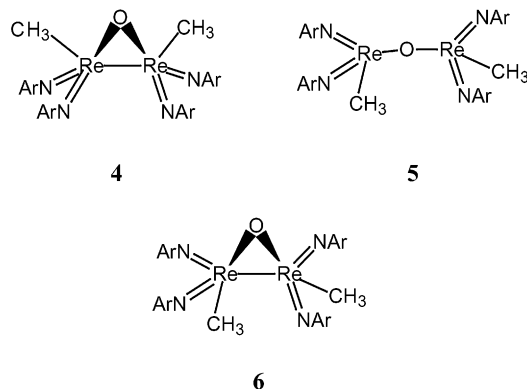
(19) Johnson, M. J. A.; Lee, P. M.; Odom, A. L.; Davis, W. M.; Cummins, C. C. *Angew. Chem., Int. Ed. Engl.* **1997**, 36, 87.

(20) Eller, P. G.; Bradley, D. C.; Hursthouse, M. B.; Meek, D. W. *Coord. Chem. Rev.* **1977**, 24, 1.

(21) Cummins, C. C. *Prog. Inorg. Chem.* **1998**, 47, 685.

(22) Williams, D. S.; Schrock, R. R. *Organometallics* **1993**, 12, 1148.

plausible formulation for the intermediate, suggesting that it may be **6**, the anti,syn analogue of **2**.



If **6** is indeed the precursor to **4**, then the ring-opened **5** might well intervene, as in $6 \rightarrow 5 \rightarrow 4$, under the presumption that Re–Re bond opening in **6** is rate controlling and that internal rotation in **5** is relatively rapid. The rate of conversion of the intermediate to **2** has a $t_{1/2}$ of roughly 1 day, so ΔG^\ddagger is about 100 kJ mol^{−1}. Relatively few comparisons are possible. Thermal reactions of metal–metal dimers have been observed and estimates made for the BDE of the M–M bonds, such as Re₂(CO)₁₀ (180 kJ mol^{−1}),²³ and the very labile cases of {C₅H₅Cr(CO)₃}₂ (6.2 kJ mol^{−1}) and {C₅Me₅Cr(CO)₃}₂ (19 kJ mol^{−1}).

Comparison of Oxo- and Sulfur-Transfer Reactions.

Both {MeRe(NAr)₂O}₂²⁴ and {MeRe(NAr)₂S}₂⁷ are dimeric in the solid state. They react with phosphines to give MeRe(NAr)₂(PZ₃)₂ and the corresponding phosphine oxides and sulfides, respectively. The reactivity of PMe_nPh_{3−n} toward {MeRe(NAr)₂O}₂ and {MeRe(NAr)₂S}₂ increases as *n* changes from 1 to 3. Also, steric effects were found to play an important role in both oxo- and sulfur-transfer reactions. Despite the similarities between {MeRe(NAr)₂O}₂ and {MeRe(NAr)₂S}₂, certain differences regarding these two species and the corresponding atom-transfer reactions are worth noting. The oxo compound exists predominantly in

the monomeric form in toluene solution at room temperature;²⁴ however, we believe that the sulfur analogue {MeRe(NAr)₂S}₂ (**1**) remains as a dimer in solution.⁷ The kinetic data for the reactions of monodentate phosphines with **1**, with a second-order dependence on [PZ₃], are clearly different from those with MeRe(NAr)₂O, which show a first-order dependence on [PZ₃]. The second-order dependence on phosphines for the reactions with **1** supports our conclusion that **1** is a dimer in solution. For dmpe and dmpm, and even for PMe₃ and PMe₂Ph (different units for the rate constants), sulfur transfer is much faster than oxo transfer. Unlike the oxo-transfer situation, the π -acidity of phosphines seems not to be the main factor in sulfur transfer. The reaction of MeRe(NAr)₂O with P(OMe)₂Ph is over 3×10^5 times faster than the reaction with PMe₂Ph. This remarkable effect of the alkoxyl group in phosphines on the oxo-transfer reaction was not observed in the analogous sulfur reaction, possibly resulting from the divergence of bridging sulfur versus terminal oxo. The basicity and steric bulkiness of the phosphines are more important than π -acidity in the sulfur-transfer reaction.

Another interesting point to make is that only **1** reacts with isocyanides to yield MeRe(NAr)₂(RNC)₂ and RNCS. The reaction of MeRe(NAr)₂O with isocyanides does not occur under the same conditions. The bond dissociation energies for RNC=O and RNC=S differ by about 60 kcal mol^{−1}, similar to the difference between R₃P=O and R₃P=S.^{25,26} Thus, a rhenium–sulfur bond, being weaker than a rhenium–oxygen bond, is likely to give rise to the different reactivities of isocyanides toward oxo- and thio-transfer reactions.

Acknowledgment. This research was supported by a grant from the National Science Foundation. Some experiments were conducted with the use of the facilities of the Ames Laboratory. We are grateful to Dr. Cole-Hamilton at the University of St. Andrews for providing the detailed synthetic procedure for Me₂P(O)CH₂PMe₂.

Supporting Information Available: X-ray crystallographic tables and NMR data. This material is available free of charge via the Internet at <http://pubs.acs.org>.

IC0255196

(23) Chernova, V. I.; Sheiman, M. S.; Rabinovich, I. B.; Syrkina, V. G. *Tr. Khim. Khim. Tekhnol.* **1973**, 43–44.

(24) Herrmann, W. A.; Ding, H.; Kühn, F. E.; Scherer, W. *Organometallics* **1998**, 17, 2751.

(25) Benson, S. W. *Chem. Rev.* **1978**, 78, 23.

(26) Gilheany, D. G. In *The Chemistry of Organophosphorus Compounds*; Hartley, F. R., Ed.; Wiley: New York, 1992; Vol. 2, p 1.